

Numerical and Experimental Analysis of the p53-mdm2 Regulatory Pathway

Ingeborg M.M. van Leeuwen^{1,2}, Ian Sanders¹, Oliver Staples¹,
Sonia Lain^{1,2}, and Alastair J. Munro¹

¹ Surgery and Oncology, Ninewells Hospital, University of Dundee, DD1 9SY
Dundee, UK

ingeborg@maths.dundee.ac.uk

² Microbiology, Tumor and Cell Biology, Karolinska Institute,
SE-17177 Stockholm, Sweden

Abstract. The p53 tumour suppressor plays key regulatory roles in various fundamental biological processes, including development, ageing and cell differentiation. It is therefore known as “the guardian of the genome” and is currently the most extensively studied protein worldwide. Besides members of the biomedical community, who view p53 as a promising target for novel anti-cancer therapies, the complex network of protein interactions modulating p53’s activity has captivated the attention of theoreticians and modellers due to the possible occurrence of oscillations in protein levels in response to stress. This paper presents new insights into the behaviour of the p53 network, which we acquired by combining mathematical and experimental techniques. Notably, our data raises the question of whether the discrete p53 pulses in single cells, observed using fluorescent labelling, could in fact be an artefact. Furthermore, we propose a new model for the p53 pathway that is amenable to analysis by computational methods developed within the OPAALS project.

Keywords: Mathematical modelling, Systems Biology, Oscillations, Pulses, Cell Cycle, Cancer.

1 Introduction

Oscillating systems in living organisms are mathematically tractable and, through analysis and understanding of their behaviour, might provide useful insights into the design of computer systems. It therefore seemed appropriate for us, as biologists within the OPAALS project, to look critically at oscillating systems in biology to see whether or not they might be used to inform the computer science aspects of the project. This paper is part of a research framework that is documented in the following four companion papers at this same conference:

- A Research Framework for Interaction Computing [15]
- Lie Group Analysis of a p53–mdm2 ODE Model [24]
- Transformation Semigroups as Constructive Dynamical Spaces [17]
- Towards Autopoietic Computing [10]

2 Oscillations in Biology

Since autopoiesis is one of OPAALS's key areas of interest, and since the archetypical autopoietic entity is the cell, we have looked systematically at sub-cellular systems that oscillate. An oscillating system can be defined as one whose attributes rise and fall in a regular fashion over a sustained period. Such systems have interesting implications for computer science: each oscillation could be regarded as the tick of a digital clock, a pulse that might be counted.

Probably the most obvious role for self-sustaining cellular oscillators in biology is as timekeepers, controlling events such as circadian rhythms [45] and embryonic development [7]. However cellular oscillators are not limited to time-keeping. Experimental as well as theoretical work has demonstrated that cellular oscillators might be capable of performing a wide variety of important functions [20]. Among them are making decisions concerning the fate of a cell [2]; controlling of calcium-dependent signalling pathways; facilitating cellular responses to changes in environment; and regulating cellular energy production [8].

2.1 The p53/mdm2 Network as an Oscillating (?) System

We have chosen to investigate the behaviour of the p53/mdm2 system. Mainly because it is a critical element in determining the fate of a cell [29] – with obvious analogies to the success (or failure) of an enterprise – and because it is one with which we are somewhat familiar. We also believed, on the basis of previously published work [4, 19, 28, 27], that oscillatory behaviour was characteristic of the system and that, by further exploring these oscillations, we could usefully contribute to the mathematical and computer science aspects of the OPAALS project. P53 is a protein that is activated in response to stress or damage to a cell and has variable effects on cellular behaviour: cells may rest and repair the damage; they may die via programmed cell death (apoptosis); they may continue to behave as normal but, later, prove incapable of division (premature replicative senescence). P53 is negatively regulated by mdm2 (murine double minute 2) – mdm2 is an enzyme that targets p53 for degradation and elimination via a process termed ubiquitination. By convention, the human homologue of mdm2 is termed hdm2.

As a first step we sought to justify some of the assumptions underlying the published work on sustained oscillations in the p53/mdm2 system. The single – cell experiments [28], upon which an elaborate mathematical superstructure has been built [1, 5, 12, 13, 19, 27, 32, 36, 38], used fluorescent labelling to monitor simultaneous changes in the levels of p53 and mdm2 following irradiation. A key assumption in any such experimental system is that the labelling does not have any effect upon the function of the protein. Our own experimental work shows that, somewhat unexpectedly, the labelling of mdm2 renders it functionally inactive. This raises the possibility that the oscillations observed in the single–cell fluorescence experiments might be an artefact caused by the labelling procedure.

2.2 Experimental Data

The Western blots shown in Figure 1 illustrate this point. A Western blot is a gel-based method for assessing the amounts of specific proteins present in an

experimental system. The darker the band, the more protein is present. The gels in the top half of the figure show the levels of unlabelled hdm2 and p53 in cells transfected with different amounts of expression plasmids for wild-type p53 and hdm2. Normal hdm2 down-regulates p53 and, as expected, we observe lower p53 levels in the presence of hdm2 (right-hand blue box) than in the absence of hdm2 (left-hand blue box). When the experiment is repeated with hdm2 labelled with yellow fluorescent protein (hdm2-YFP), however, the outcome is different. In the lower pair of gels in Figure 1 there is, if anything, more p53 expression within the blots enclosed by the right-hand box. This suggests strongly that labelling of hdm2 might impair its ability to down-regulate p53 expression.

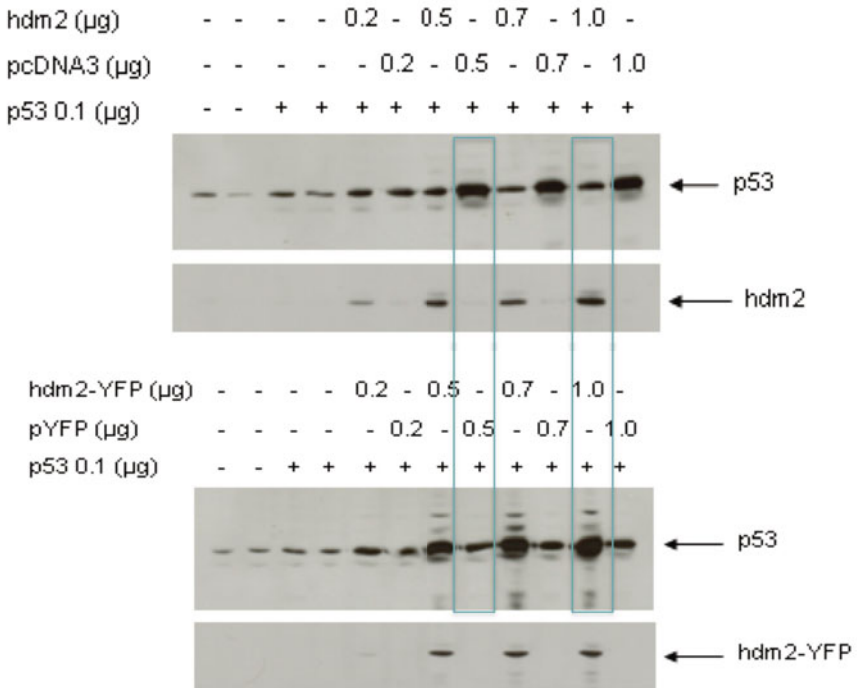


Fig. 1. MCF-7 cells were transiently transfected with hdm2 or hdm2-YFP (pU293), and as controls pcDNA3 or pYFP were also transfected in a gradient. In addition p53 wild-type (0.1µg) plasmid was transfected as indicated. In the lower gel there is abundant p53 (right-hand blue box) despite presence of hdm2. If the labelled hdm2 were functional we would expect to see inhibition of p53 but, if anything, p53 is induced.

It is possible that the sustained oscillations that have been observed in single-cell experiments may be due to artefacts induced by the abnormalities in mdm2 function introduced by the labelling procedure. This leaves us somewhat sceptical concerning the ability of regular sustained oscillations in the p53/mdm2 system, within individual cells, to act as a digital counting mechanism for determining the fate of a cell.

Nevertheless we have good evidence from our own work (e.g. Figure 2) and that of others [30] that the p53/mdm2 system can oscillate in response to irradiation – but that these oscillations are damped. There are several possible explanations for such damped oscillations – the most parsimonious is that p53 and MDM2 operate in a simple feedback loop but with a discrete time delay [34]. Another explanation – less favoured by us for the reasons given – is that the damping at the aggregate level is caused by the presence of a mixed population of cells.

Having set out to use sustained oscillations in the p53/mdm2 system as the basis of our mathematical models we were forced into an unexpected conclusion: close scrutiny of some so-called “oscillating systems” shows that the biological observations upon which they are based may be flawed and, furthermore, the models used to demonstrate oscillations may only show oscillatory behaviour under certain restricted and somewhat artificial conditions. The literature at the interface between mathematics and biology is not as robust as a superficial reading would lead us to believe. Perhaps this is a reflection of a more general problem in interdisciplinary research: it is difficult to achieve a balance of expertise. Mathematical sophistication can be undermined by biological naïveté, and *vice versa*.

Our disappointment with our initial exploration of oscillating systems raises a fairly fundamental question: when we are using natural science to influence mathematics, algebra and computer science, are we seeking to inspire using a model that accurately reflects the natural world, a robust template; or are we simply generating possibilities, initiating chains of thought and encouraging creative approaches? If our aim is the latter then the extent to which our models fit the biological observations is less than critical – indeed could be entirely unimportant; if our aim is the former, then the goodness-of-fit is crucial. At this point it seems entirely reasonable to leave the question rhetorical, unanswered.

Despite our concerns about *sustained* oscillations in the p53/mdm2 system we are confident that the p53/mdm2 system exhibits *damped* oscillations in cell populations, as shown in Figure 2. This information has been used to inform the mathematical models that are discussed in the following section.

3 Mathematical Modelling of the p53 Network

During the cell cycle, key proteins undergo cyclic synthesis and degradation, the associated changes in their levels triggering progression through the cell-cycle phases. In recent years, similar oscillatory behaviour has been shown in several other regulatory networks. The NF- κ B transcription factor, for instance, presents sustained nucleo-cytoplasmic fluctuations after stimulation with TNF α [3, 25, 35]. Similarly, the levels of Hes1 protein and mRNA oscillate in cell culture upon serum treatment [6, 23]. In the mouse segmentation clock, not only the levels of Hes1 but also of components of the Wnt and Notch pathways have been shown to oscillate *in vivo* [14, 49]. Given the biomedical importance of these pathways, the molecular basis and biological implications of their oscillations have attracted extensive attention from experimentalists and theoreticians alike. Although the signalling pathways above differ in their components and biological outcomes, the oscillations are believed to

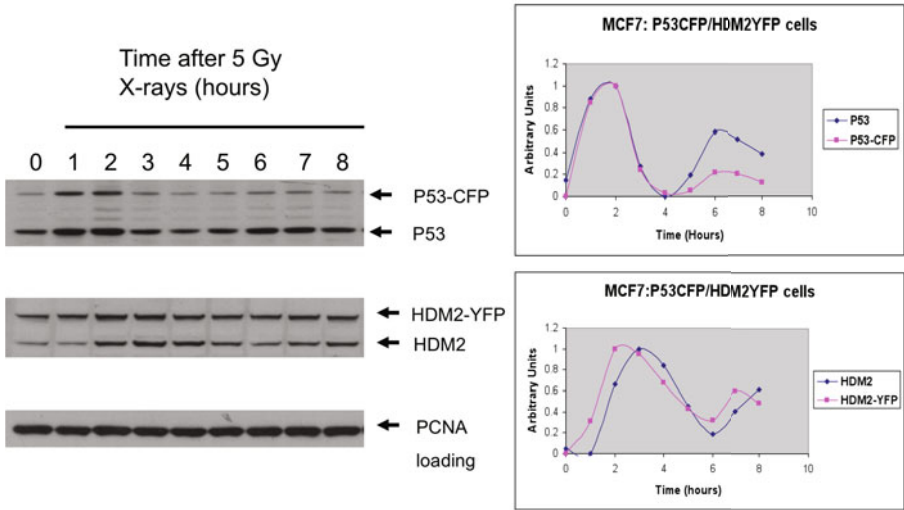


Fig. 2. Levels of p53 and mdm2 after irradiation of cells in suspension. There is a prominent peak for p53 at 2 hours post exposure followed by a second (lower) peak at 6 hours; for mdm2 the peaks are at 3 hours and 7 hours. Findings consistent with a delay between the rise in p53 and the induction of mdm2. Each observation is based on a pooled estimate from > 100, 000 cells; the error bars (s.e.m.) are very narrow and are obscured by the data points themselves.

share a common underlying mechanism: a negative feedback loop (NFL) combined with a transcriptional delay [34, 37, 44]. Notably, such a mechanism is present in the p53–mdm2 network (Figure 3), as p53 promotes the synthesis of its main negative regulator, mdm2 (Figure 4). The possibility that p53 levels oscillate in response to stress has therefore been explored both experimentally and theoretically.

The p53 pathway has been subject to extensive modelling efforts, the first model being published by Bar-Or and co-workers in 2000. The existing models can be classified into two categories based on their purpose. On the one hand, relatively simple models describing the role of p53 in cancer have been developed as part of multiscale models for the disease [11, 16, 31, 40]. Ribba *et al.* [40], for instance, used p53 as a switch adopting values 0 and 1 in the absence and presence of DNA damage, respectively, whereas in the cellular automaton model developed by Alarcon and co-workers [11] cells possess different automaton features depending on whether their p53 status is wild-type or mutant. On the other hand, various kinetic models have been built to investigate whether the system can give rise to damped oscillations in p53 and mdm2 in cell populations and un-damped pulses in individual cells [1, 5, 9, 13, 19, 28, 32, 33, 34, 30, 38, 39, 48, 51]. The vast majority assume that a cell consists of a single compartment in which the proteins of interest are abundant and evenly distributed; hence they undertake a continuum, deterministic approach, using either ordinary or delay differential equations (ODEs or DDEs) to describe the changes in protein levels. Alternative modelling approaches include stochastic, spatial and multiple compartment models. Proctor *et al.* [38], for instance, developed

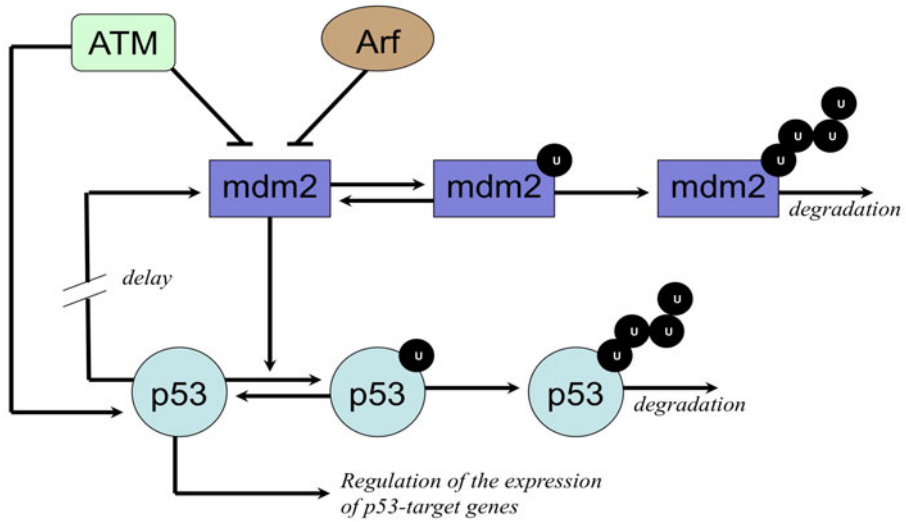


Fig. 3. Simple schematic of the p53 network. The p53 tumour suppressor – the guardian of the genome – acts as a transcription factor, regulating the expression of over a hundred target genes [18, 29, 47]. The mdm2 protein, a RING finger-dependent ubiquitin protein ligase, binds to p53 and targets it for proteasomal degradation [22]. Both p53 and mdm2 are highly regulated proteins [26].

stochastic models to account for the intercellular variation in the number of macromolecules. In contrast, Ciliberto *et al.* [13] formulated a deterministic, compartmental ODE model that distinguishes between nuclear and cytoplasmic mdm2. Finally, Gordon *et al.* [21] relaxed the intracellular homogeneity assumption further and used partial differential equations (PDEs) to describe intracellular protein density patterns.

To prevent the negative feedback loop linking p53 and mdm2 (Figure 4) from immediately inhibiting itself and, in particular, to enable oscillations to occur, a delay in the negative feedback loop is required [43]. Such a delay can be modelled in different ways. In some cases the delay has been included implicitly in mathematical models – Lev Bar-Or *et al.* [30], for instance, included an additional unknown component in the p53–mdm2 pathway, whereas Ciliberto *et al.* [13] combined positive and negative feedbacks. The alternative is to incorporate time delays explicitly. Srividya *et al.* [42] have shown that discrete delay terms can help reduce the number of variables and parameters required to describe a molecular system by replacing one or more intermediate reactions. Concerning spatial effects, [34] demonstrated that the waiting times associated with transcription and translation can be fused into a single time delay without altering the dynamical properties of the system. Hence, several models [5, 21, 34, 36] calculate the rate of mdm2 synthesis at time t as a function of the amount of p53 present in the system at time $t - \tau$.

Below we discuss in detail three existing theoretical approaches to the p53 pathway (i.e. [30, 34, 13]), while in the next section we present a new model. To facilitate

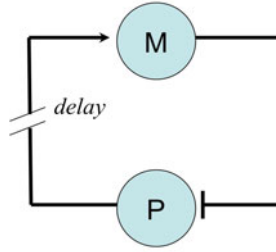


Fig. 4. Negative feedback loop with transcriptional delay linking p53 and mdm2

comparison of the models, we have unified the notation as follows: $[P(t)]$ and $[M(t)]$ are the total intracellular concentrations of p53 and mdm2 at time t ; $S(t)$ represents a transient stress stimulus (e.g. DNA damage); s_* are *de novo* synthesis rates; k_* are production rates (e.g. phosphorylation); j_* are reverse reactions (e.g. desphosphorylation); d_* are degradation rates; σ_* are transport rates; K_* are saturation coefficients and c_* are additional constants.

3.1 Model I: Lev Bar-Or et al. (2000)

The first model for the p53-mdm2 network, formulated by Lev Bar-Or *et al.* [30], describes the interaction between p53 and mdm2. The time-lag between p53 activation and p53-mediated induction of mdm2 synthesis is modelled by the presence of a hypothetical intermediary, X . The proposed kinetic equations are [30]:

$$\begin{aligned}
 d[P]/dt &= s_p - \left(d_p + \widehat{d}_{pm}(t)[M] \right) [P], \\
 d[M]/dt &= s_{m0} + \frac{s_{mx}[X]^n}{[X]^n + K_{mx}^n} - d_m[M], \\
 d[X]/dt &= \frac{s_s S(t)[P]}{1 + c_x[M][P]} - d_x[X],
 \end{aligned}
 \tag{1}$$

with initial conditions $[P(0)] = P_0$, $[M(0)] = M_0$, and $[X(0)] = 0$. The stress stimulus S is assumed to influence the behaviour of the system in two ways, namely by promoting p53’s transcriptional activity and by downregulating mdm2-mediated degradation of p53. The former mechanism is modelled by making the synthesis of X an increasing function of S , while the latter is incorporated by making \widehat{d}_{pm} a decreasing function of S . Numerical analyses and simulations revealed that, for certain parameter values, the system can show damped oscillations in which mdm2 and p53 levels peak out of phase.

3.2 Model II: Monk (2003)

In contrast to [30], the model proposed by Monk [34] not only characterizes the dynamics of the mdm2 and p53 proteins, but also the changes in the level of mdm2 mRNA. Moreover, it explicitly accounts for a transcriptional delay as follows:

$$\begin{aligned}
 d[P]/dt &= s_p - \left(d_{p0} + \frac{d_{pm2}[M]^2}{[M]^2 + K_{pm}^2} \right) [P], \\
 d[R_M]/dt &= s_{rm0} + \frac{s_{rm1}[P(t-\tau)]^n}{[P(t-\tau)]^n + K_{rm}^n} - d_{rm}[R_M], \\
 d[M]/dt &= s_{rt}[R_M] - d_m[M],
 \end{aligned} \tag{2}$$

where both p53's transcriptional activity and mdm2's ubiquitin-ligase activity are assumed to be saturating functions. The system demonstrates oscillatory behaviour for certain parameter values, the period of the oscillations depending on the transcriptional delay and the protein and mRNA half-lives.

3.3 Model III: Ciliberto et al. (2005)

Compared with the approaches above, Ciliberto *et al.* [13] incorporated substantially more biological detail in their model, to arrive at a relatively more sophisticated description of the p53–mdm2 network that accounts for two subcellular compartments, namely the nucleus and the cytoplasm. As it is assumed that mdm2 has to be phosphorylated in order to enter the nucleus, the model includes three molecular forms of mdm2: nuclear mdm2, and both unphosphorylated and phosphorylated cytoplasmic mdm2. Moreover, ubiquitination is modelled as a multistep process (Figure 3), involving three molecular forms of p53 (i.e., non-ubiquitinated, mono-ubiquitinated and poly-ubiquitinated protein). The dynamics of the six molecular components is expressed by:

$$\begin{aligned}
 d[P]/dt &= s_p - d_p[P] - d_{pu}[PUU], \\
 d[P_U]/dt &= k_u([P] - [P_U] - [PUU])[M_N] + j_u[PUU] \\
 &\quad - (j_u + d_{p1} + k_u[M_N])[P_U], \\
 d[PUU]/dt &= k_u[M_N][P_U] - (j_u + d_{pu} + d_{p1})[PUU], \\
 d[M_N]/dt &= (\sigma_{cn}[M_{PC}] - \sigma_{nc}[M_N])v - \left(d_{m0} + \frac{d_{m1}\mathcal{S}(t)}{\mathcal{S}(t) + K_m} \right) [M_N], \\
 d[M_C]/dt &= s_{m0} + \frac{s_{m1}[P]^n}{[P]^n + K_{pm}^n} + k_{pc}[M_{PC}] - \left(d_{m0} + \frac{k_{pc}}{[P] + K_{pc}} \right) [M_C], \\
 d[M_{PC}]/dt &= \frac{k_{pc}[M_C]}{[P] + K_{pc}} + \sigma_{nc}[M_N] - (j_{pc} + \sigma_{cn} + d_{m0})[M_{PC}],
 \end{aligned} \tag{3}$$

The state variables above represent the concentrations of total p53, P ; monoubiquitinated p53, P_U ; poly-ubiquitinated p53, PUU ; nuclear mdm2, M_N ; unphosphorylated cytoplasmic mdm2, M_C ; and phosphorylated cytoplasmic mdm2, M_{PC} . The parameter v denotes the nuclear-cytoplasmic volume ratio. Unlike in the previous models, the value of the stress function \mathcal{S} depends on the level of p53, as it is assumed that p53 plays a role in DNA repair:

$$d\mathcal{S}/dt = \widehat{k}_s(I(t)) - \frac{d_s\mathcal{S}(t)[P]}{\mathcal{S}(t) + K_s},$$

where \widehat{k}_s is the DNA damage production rate as a function of time and dose of irradiation. Based on numerical analyses and simulations, the authors suggest that the discrete pulses observed by Lahav *et al.* [28] might be the result of a combination of positive and negative feedbacks. In the model, *the positive feedback originates from two opposing negative effects: nuclear mdm2 induces p53 degradation, while p53 inhibits nuclear entry of mdm2, by inhibiting phosphorylation of mdm2 in the cytoplasm. The negative feedback loop is the well-known fact that p53 induces the synthesis of mdm2* [13].

Eqns (3) also predict that the level of mdm2 can increase in the absence of mdm2 synthesis, which indicates a mass balance problem. This can be solved by rewriting the expressions for the changes in $[M_N]$ and $[M_{PC}]$:

$$\begin{aligned} d[M_N]/dt &= v\sigma_{cn}[M_{PC}] - \sigma_{nc}[M_N] - \left(d_{m0} + \frac{d_{m1}\mathcal{S}(t)}{\mathcal{S}(t) + K_m} \right) [M_N], \\ d[M_{PC}]/dt &= \frac{k_{pc}[M_C]}{[P] + K_{pc}} + \frac{\sigma_{nc}[M_N]}{v} - (j_{pc} + \sigma_{cn} + d_{m0})[M_{PC}]. \end{aligned} \quad (4)$$

An analogous modification has been introduced in [1], which presents a four ODE model inspired by [13]. The new system of ODEs based on (4) does not oscillate for the parameter values used in [13].

4 Formulation of the New Model

To show that there is yet another possible biological explanation for the occurrence of oscillations in p53 levels in response to stress, we will now introduce a new model for the p53 pathway, which we will refer to as Model IV. The structure of our simple network is shown in Figure 6. It describes the interactions between four molecular components: P_I , the p53 tumour suppressor, M , p53's main negative regulator, mdm2, C , the p53–mdm2 complex and, P_A , an *active* form of p53 that is resistant against mdm2-mediated degradation. The model accounts for the following phenomena: (1) basal p53 synthesis; (2) basal (i.e. mdm2-independent) p53 degradation; (3) mdm2 synthesis; (4) basal mdm2 degradation; (5) p53–mdm2 complex assembly; (6) p53–mdm2 complex dissociation; (7) mdm2-mediated p53 ubiquitination and subsequent elimination; (8) stress-induced p53 activation; (9) p53 inactivation; and (10) basal degradation of active p53. According to the reaction scheme shown in Figure 6, the changes in the concentrations of the four molecular components are given by:

$$\begin{aligned} d[P_I]/dt &= r_1 - r_2 - r_5 + r_6 - r_8 + r_9, \\ d[M]/dt &= r_3 - r_4 - r_5 + r_6 + r_7, \\ d[C]/dt &= r_5 - r_6 - r_7, \\ d[P_A]/dt &= r_8 - r_9 - r_{10}. \end{aligned} \quad (5)$$

where $r_i(t)$, for $i = 1, \dots, 10$, is the rate of reaction i at time t and $[X]$ denotes the concentration of molecular component X , for $X = P_I, P_A, M$, and C .

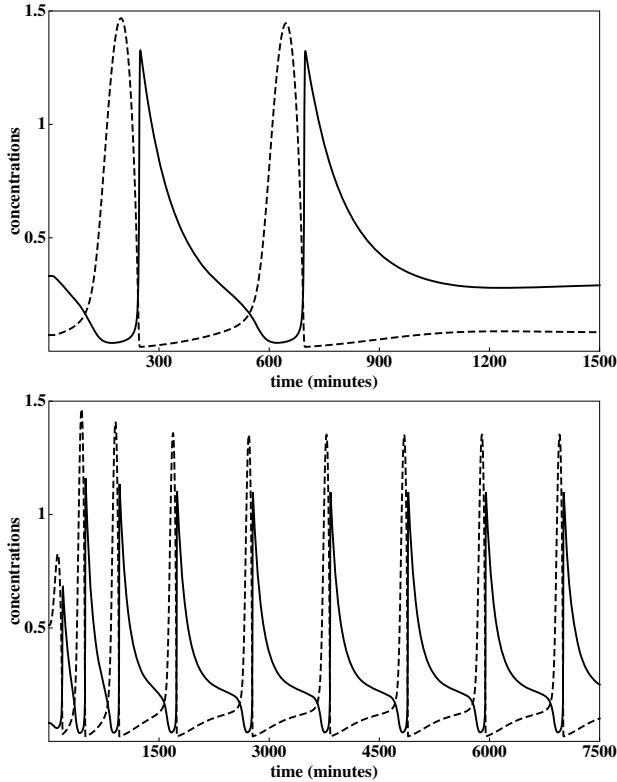


Fig. 5. Simulations with the original model by Ciliberto *et al.* [13] (Eqns (3)) showing two pulses (*left*) and sustained oscillations (*right*) in the levels of total p53, $[P]$ (dashed lines), and nuclear mdm2, $[MN]$ (solid lines). For the parameter values, see the original paper [13]. In the left and right panels, the value of the cytoplasm:nucleus ratio, v , is 15 and 11, respectively.

4.1 Simplifying Assumptions

For simplicity, we assume that the basal p53 synthesis rate, r_1 , remains constant in time and that basal degradation rates, r_2 , r_4 and r_{10} , are proportional to the corresponding substrate concentrations. The mdm2 protein, a RING finger-dependent ubiquitin protein ligase, is known to bind to p53 and target it for proteasomal degradation [22]. In the model, the binding of mdm2 to p53 is assumed to be reversible with assembly and dissociation rates r_5 and r_6 , respectively. Furthermore, experimental evidence has shown that mdm2's downregulation of p53 is inhibited under DNA damage [41]. We have incorporated this observation into the model by assuming that ionising radiation induces the phosphorylation of p53, which prevents mdm2 binding. That is, r_8 is an increasing function of the level of radiation exposure. Finally, reaction 3 represents the negative feedback loop in which p53 transactivates expression of the *MDM2* gene [50]. As we expect this expression rate to reach a maximum value when there is negligible delay between the binding of two successive

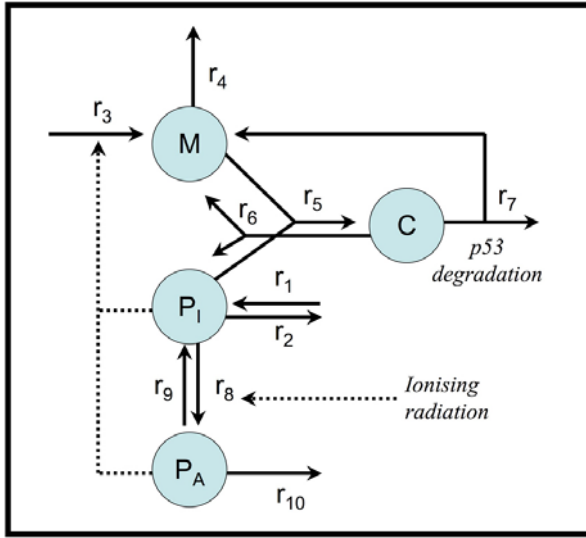


Fig. 6. Schematic of the new p53-mdm2 interaction model. M = mdm2 protein; PI = inactive p53 protein, C = mdm2-p53 complex; PA = active p53 protein.

p53 molecules to the *MDM2* promoter region, we assume that r_3 is a saturating function of the total level of p53. Given the assumptions above, the reaction rates can be calculated as follows:

$$\begin{aligned}
 r_1(t) &= s_p, \\
 r_2(t) &= d_p[P_I(t)], \\
 r_3(t) &= s_{m0} + \frac{s_{m1}[P_I(t)] + s_{m2}[P_A(t)]}{[P_I(t)] + [P_A(t)] + K_m}, \\
 r_4(t) &= d_m[M(t)], \\
 r_5(t) &= k_c[P_I(t)][M(t)], \\
 r_6(t) &= j_c[C(t)], \\
 r_7(t) &= k_u[C(t)], \\
 r_8(t) &= k_a\mathcal{S}(t)[P_I(t)], \\
 r_9(t) &= j_a[P_A(t)], \\
 r_{10}(t) &= d_p[P_A(t)].
 \end{aligned}$$

Substitution of the expressions above into Eqns (5) yields:

$$\begin{aligned}
 d[P_I]/dt &= s_p + j_a[P_A] - (d_p + k_a\mathcal{S}(t))[P_I] - k_c[P_I][M] + j_c[C], \\
 d[M]/dt &= s_{m0} + \frac{s_{m1}[P_I] + s_{m2}[P_A]}{[P_I] + [P_A] + K_m} + k_u[C] + j_c[C] - (d_m + k_c[P_I])[M], \\
 d[C]/dt &= k_c[P_I][M] - (j_c + k_u)[C], \\
 d[P_A]/dt &= k_a\mathcal{S}(t)[P_I] - (j_a + d_p)[P_A].
 \end{aligned}$$

4.2 Model IV: Dimensionless Equations

The state variables in Figure 6 can be scaled as

$$\begin{aligned} P_i &= k_u[P_I]/s_p, \\ M &= k_u[M]/s_p, \\ C &= k_u[C]/s_p, \\ P_a &= k_u[P_A]/s_p \text{ and} \\ \tau &= k_u t. \end{aligned}$$

In terms of these new variables, the model equations reduce to:

$$\begin{aligned} dP_i/d\tau &= 1 + \beta_a P_a - (\beta_p + \alpha_a S(\tau))P_i \\ &\quad - \alpha_c P_i M + \beta_c C, \end{aligned} \quad (6)$$

$$\begin{aligned} dM/d\tau &= \alpha_{m0} + \frac{\alpha_{m1}P_i + \alpha_{m2}P_a}{P_i + P_a + \kappa_m} + C \\ &\quad - (\beta_m + \alpha_c P_i)M + \beta_c C, \end{aligned} \quad (7)$$

$$dC/d\tau = \alpha_c P_i M - (1 + \beta_c)C, \quad (8)$$

$$dP_a/d\tau = \alpha_a S(\tau)P_i - (\beta_a + \beta_p)P_a. \quad (9)$$

where the dimensionless parameters are defined as:

$$\begin{aligned} \alpha_a &= k_a/k_u, \\ \beta_a &= j_a/k_u, \\ \alpha_c &= k_c s_p/k_u^2, \\ \beta_c &= j_c/k_u, \\ \alpha_{m0} &= s_{m0}/s_p, \\ \alpha_{m1} &= s_{m1}/s_p, \\ \alpha_{m2} &= s_{m2}/s_p, \\ \beta_m &= d_m/k_u, \\ \beta_p &= d_p/k_u \text{ and} \\ \kappa_m &= k_u K_m/s_p. \end{aligned}$$

In the simulations depicted in Figure 7, two modes of stress have been considered, namely a discrete pulse insult at time zero and long-term exposure to a constant stressful stimulus. The former is expressed as:

$$S(t) = e^{-c_s t} \quad \text{and} \quad S(\tau) = e^{-\gamma \tau}, \quad (10)$$

in dimensional and dimensionless form, respectively (the dimensionless stress coefficient is $\gamma = c_s/k_u$). In contrast, the latter is modelled as:

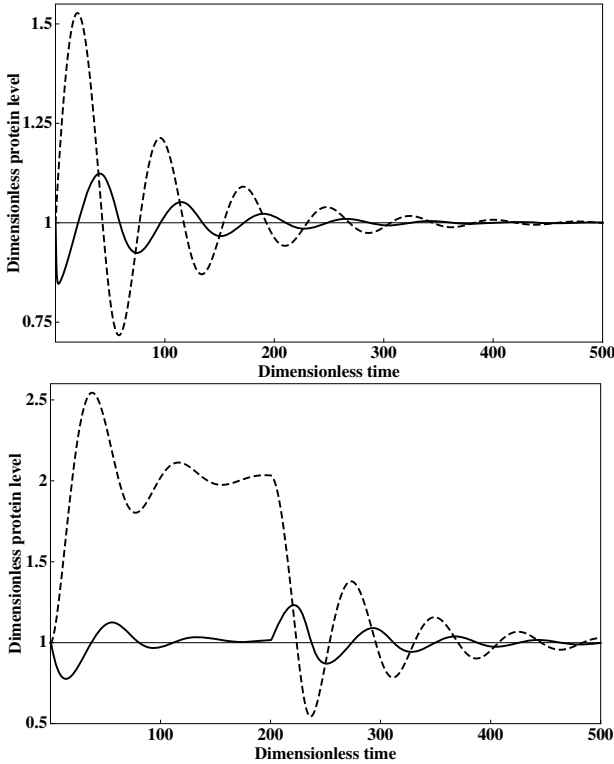


Fig. 7. Simulations with the dimensionless system (6–9) showing damped oscillations in the levels of total p53, P_i+P_a+C (dashed lines), and total mdm2, $M+C$ (solid lines). The values have been normalised with respect to the corresponding concentrations in the absence of stress (i.e., $P_{i0}+C_0$ and M_0+C_0 , respectively). The parameter values used in the simulations are provided in Table 1. One dimensionless time unit corresponds to 2.5 minutes. *Left panel* : response to a single pulse insult at time $\tau = 0$ (Eqn (10) with $\gamma = 2.5$). *Right panel* : response to a constant, long-term insult (Eqn (11) with $\gamma = 2.5$, $\tau_i = 200$ and $S_0 = 0.05$).

$$\begin{aligned}
 S(\tau) &= S_0 & \text{for } 0 \leq \tau \leq \tau_i \\
 &= S_0 e^{-\gamma(\tau-\tau_i)} & \text{for } \tau > \tau_i.
 \end{aligned}
 \tag{11}$$

Notably, the response of the system to the two kinds of insult is very different. Exposure to a single, pulse insult at time zero results in damped oscillations in the levels of p53 and mdm2 around their steady-state values in the absence of stress. In contrast, exposure to a long-term signal causes the system to move to a new steady-state, fluctuating transiently. This new steady-state has a higher p53 level, which depends on the strength of the signal. When the stimulus ends, the system returns to its original steady-state, displaying a second round of damped oscillations.

Table 1. Parameter values used in the model simulations shown in Figure 7

$[P_I(0)] = 9.42 \text{ nM}$	$k_a = 20 \text{ min}^{-1}$
$[P_A(0)] = 0 \text{ nM}$	$k_c = 4 \text{ min}^{-1} \text{ nM}^{-1}$
$[C(0)] = 3.49 \text{ nM}$	$k_u = 0.4 \text{ min}^{-1}$
$[M(0)] = 0.037 \text{ nM}$	$j_a = 0.2 \text{ min}^{-1}$
$s_{m0} = 2 \times 10^{-3} \text{ nM/min}$	$j_c = 2 \times 10^{-3} \text{ min}^{-1}$
$s_{m1} = 0.15 \text{ nM/min}$	$s_p = 1.4 \text{ nM/min}$
$s_{m2} = 0.2 \text{ nM/min}$	$d_p = 2 \times 10^{-4} \text{ min}^{-1}$
$d_m = 0.4 \text{ min}^{-1}$	
$K_m = 100 \text{ nM}$	
$P_{i0} = 2.69$	$\alpha_a = 50$
$P_{a0} = 0$	$\alpha_c = 35$
$C_0 = 1.0$	
$M_0 = 0.01$	$\beta_a = 0.5$
$\alpha_{m0} = 0.00143$	$\beta_c = 5 \times 10^{-3}$
$\alpha_{m1} = 0.107$	
$\alpha_{m2} = 0.143$	$\beta_p = 5 \times 10^{-4}$
$\beta_m = 1$	
$\kappa_m = 28.57$	

5 Discussion

In the above section we have visited four alternative mathematical descriptions of the p53 network. Their specific features are highlighted in Table 2. These models, which represent only a small sample of the models available in the literature, were chosen to illustrate the use of differential equations in systems biology and, in particular, to show how very different mechanisms can succeed in explaining the same data. The modelling efforts addressed here were motivated mainly by two experimental studies. First, Lev Bar-Or *et al.* [30] exposed mouse fibroblasts NIH 3T3 cells expressing wild-type p53 and mdm2 to 5 Gy of irradiation and then measured the protein levels at several time points after exposure. Their Western Blots showed two peaks in the level of p53, each followed by a peak in mdm2 approximately one hour later. Second, Lahav and co-workers [28] created a cell line expressing p53 and mdm2 tagged with fluorescent proteins to study the dynamics of these molecules in single cells. In response to γ -radiation, they observed digital pulses in both p53 and mdm2 levels (for a critical discussion on this approach, see Section 2.2). Unifying the two experimental observations, Ma *et al.* [32] suggested that *the damped oscillations previously observed in cell populations can be explained as the aggregate behaviour of single cells*. Comparing the four models above, models I [30] and II [34] are the most similar, as they both produce an oscillatory behaviour based on the mdm2–p53 NFL (Figure 4) alone and both account for an intermediary component linking of the level of p53 to the rate of mdm2 synthesis. The main difference is that model II also includes an explicit transcriptional delay, which implies a shift of the mathematical approach from ODEs to DDEs. According to model III [13], however, the mechanism underlying the oscillations is more complex and involves both negative and positive

Table 2. Summary of the mathematical models described in this chapter

	FEATURES	MECHANISM(S) FOR OSCILLATIONS
MODEL I Lev Bar-Or <i>et al</i> [30]	<ul style="list-style-type: none"> • 3 ODEs + 1 expression for the stress function • Includes an unknown intermediary 	<ul style="list-style-type: none"> • Implicit delay, in the form of an unknown intermediary, in the mdm2-p53 negative feedback loop
MODEL II Monk [34]	<ul style="list-style-type: none"> • 2 ODEs + 1 DDE • Includes mdm2 mRNA dynamics 	<ul style="list-style-type: none"> • Implicit time delay, in the form of a known intermediary (i.e, mdm2 mRNA), in the mdm2-p53 negative feedback loop • Explicit time delay for gene transcription
MODEL III Ciliberto <i>et al</i> [13]	<ul style="list-style-type: none"> • 6 ODEs + 1 ODE for the stress function • Distinguishes between nuclear and cytoplasmic mdm2 • Accounts for 3 molecular forms of p53 and 2 forms of mdm2 • DNA damage enhances mdm2 degradation • p53 promotes DNA repair 	<ul style="list-style-type: none"> • Combination of positive and negative feed back loops between mdm2 and p53 • Implicit time delay (mdm2 has to be phosphorylated and then shuttled into the nucleus before it can degrade p53)
MODEL IV New model	<ul style="list-style-type: none"> • 4 ODEs + 1 expression for the stress function • Characterises of the dynamics of the p53-mdm2 complex • Accounts for a mdm2-resistant form of p53 	<ul style="list-style-type: none"> • mdm2-p53 negative feedback loop • p53 binding protects mdm2 from proteosomal degradation

feedbacks. In response to ionising radiation, DNA damage *increases abruptly as does* [. . .] *the rate of* [. . .] *degradation of* [M_N]. *As* [M_N] *decreases, [* P] *increases, which causes an initial drop in* [M_{PC}] *and a steady increase in* [M_C]. *When a sufficient amount of mdm2 accumulates in the cytoplasm, it initiates a change of regime: phosphorylated mdm2 enters the nucleus, causing increased degradation of p53, which relieves the inhibition of mdm2 phosphorylation in the cytoplasm, allowing more mdm2 to enter the nucleus. The positive feedback loop causes the abrupt drop in* [P] *and rise in* [M_N]. *The drop in* [P] *cuts off the synthesis of* [M_C], *and consequently* [M_C] *and* [M_N] *drop. The system is back to the original state, [* P] *starts to accumulate again due to the low level of* [M_N] *and a new oscillation starts* [13].

While model III incorporates substantially more biologically-relevant information than models I and II, its main weaknesses are the strong dependence of the behaviour of the system on the relative size of the nucleus (see the simulations in Figure 3) and the mass balance problems discussed above (see corrected Eqns (4)).

Model III predicts a decrease in nuclear mdm2 in response to stress (Figure 5), and a subsequent reduction in mdm2-mediated p53 degradation. This is also the case in the context of model IV (Figure 7). The reason behind the drop in mdm2 is different,

though. According to model III, the degradation rate of nuclear mdm2 is an increasing function of the level of DNA damage. In contrast, under model IV, p53-binding protects mdm2 from proteasomal degradation and, therefore, any decrease in [P1] translates naturally in an increased mdm2 elimination rate. Hence, when radiation promotes the transformation of P_I into P_A , mdm2 has less chance to bind to P_I and is thus at a higher risk of being rapidly degraded. This model prediction highlights the importance of accounting for the dynamics of the mdm2–p53 complex, as suggested by Proctor *et al.* [38] *since the regulation of p53 is dependent on its interaction with mdm2, we would expect that the oscillatory behaviour of the system would be strongly affected by the binding affinity of mdm2 to p53. Therefore any mechanistic model of the system should include the mdm2–p53 complex.* The reduction in mdm2 levels in response to stress in models III and IV plays a role equivalent to the transcriptional delay in models I and II: it enables the levels of mdm2 and p53 to peak out of phase, thereby allowing oscillations to occur.

The purpose of the experimental and numerical work is to gain better insight into the dynamics of the chosen cellular regulatory pathway and of the ODE models that represent it most faithfully. The next step is to derive the corresponding automaton and extract the algebraic structure of its semigroup (in OPAALS), whilst simultaneously performing the Lie group analysis of the ODE system (BIONETS). Once these more powerful analytical tools are in place, we can re-examine the models discussed in this chapter, in order to correlate algebraic structure to observed or numerically calculated behaviour.

Acknowledgements

The partial support for this work by the OPAALS (FP6-034824) EU project is gratefully acknowledged. The experimental work summarised in Figures 1 and 2 was supported by other sources (CRUK, The Ninewells Cancer Campaign, a bequest from the estate of Mrs D.B. Miller). Individuals contributing to the data presented include Elizabeth Sinclair and Johanna Campbell.

References

1. Abou-Jaude, W., Ouattara, D.A., Kaufman, M.: From structure to dynamics: Frequency tuning in the p53-mdm2 network. i. Logical approach. *J. Theor. Biol.* 258, 561–577 (2009)
2. Agrawal, S., Archer, C., Schaffer, D.V.: Computational models of the notch network elucidate mechanisms of context-dependent signaling, *PLoS. Comput. Biol.* 5, e1000390 (2009)
3. Ankers, J.M., Spiller, D.G., White, M.R.H., Harper, C.V.: Spatio-temporal protein dynamics in single living cells. *Curr. Opin. Biotechnol.* 19, 375–380 (2009)
4. Batchelor, E., Loewer, A., Lahav, G.: The ups and downs of p53: understanding protein dynamics in single cells. *Nat. Rev. Cancer* 9, 371–377 (2009)
5. Batchelor, E., Mock, C.S., Bhan, I., Loewer, A., Lahav, G.: Recurrent initiation: A mechanism for triggering p53 pulses in response to DNA damage. *Mol. Cell.* 30, 277–289 (2008)

6. Bernard, S., Cajavec, B., Pujo-Menjouet, L., Mackey, M.C., Herzl, H.: Modelling transcriptional feedback loops: the role of Gro/Tle1 in Hes1 oscillations. *Phil. Trans. R. Soc. A* 364, 1155–1170 (2006)
7. Bessho, Y., Kageyama, R.: Oscillations, clocks and segmentation. *Curr. Opin. Gen. Dev.* 13, 379–384 (2003)
8. Bier, M., Teusink, B., Kholodenko, B.N., Westerhoff, H.: Control analysis of glycolytic oscillations. *Biophys. Chem.* 62, 15–24 (1996)
9. Bottani, S., Grammaticos, B.: Analysis of a minimal model for p53 oscillations. *J. Theor. Biol.* 249, 235–245 (2007)
10. Briscoe, G., Dini, P.: Towards Autopoietic Computing. In: *Proceedings of the 3rd OPAALS International Conference, Aracaju, Sergipe, Brazil, March 22-23 (2010)*
11. Byrne, H.M., van Leeuwen, I.M.M., Owen, M.R., Alarcon, T.A., Maini, P.K.: Multiscale modelling of solid tumour growth. In: Bellomo, N., Chaplain, M.A.J., de Angelis, E. (eds.) *Selected Topics on Cancer Modelling: Genesis, Evolution, Immune Competition and Therapy. Modelling and Simulation in Science, Engineering and Technology*, Birkhauser, Boston (2008)
12. Chickarmane, V., Nadim, A., Ray, A., Sauro, H.: A p53 oscillator model of dna break repair control (2006), <http://arxiv.org/abs/q-bio.mn/0510002>
13. Ciliberto, A., Novak, B., Tyson, J.J.: Steady states and oscillations in the p53/mdm2 network. *Cell Cycle* 4, 488–493 (2005)
14. Dequeant, M.L., Glynn, E., Gaudenz, K., Wahl, M., Chen, J., Mushegian, A., Pourquie, O.: A complex oscillating network of signaling genes underlies the mouse segmentation clock. *Science* 314, 1595–1598 (2006)
15. Dini, P., Schreckling, D.: A Research Framework for Interaction Computing. In: *Proceedings of the 3rd OPAALS International Conference, Aracaju, Sergipe, Brazil, March 22-23 (2010)*
16. Dionysiou, D.D., Stamatakos, G.S.: Applying a 4D multiscale in vivo tumour growth model to the exploration of radiotherapy scheduling: the effects of weekend treatment gaps and p53 gene status on the response of fast growing solid tumors. *Cancer Informatics* 2, 113–121 (2006)
17. Egri-Nagy, A., Dini, P., Nehaniv, C.L., Schilstra, M.J.: Transformation Semigroups as Constructive Dynamical Spaces. In: *Proceedings of the 3rd OPAALS International Conference, Aracaju, Sergipe, Brazil, March 22-23 (2010)*
18. Farmer, G., Bargonetti, J., Zhu, H., Friedman, P., Prywes, R., Prives, C.: Wild-type p53 activates transcription in vivo. *Nature* 358, 83–84 (1992)
19. Geva-Zatorsky, N., Rosenfeld, N., Itzkovitz, S., Milo, R., Sigal, A., Dekel, E., Yarnitzky, T., Liron, Y., Polak, P., Lahav, G., Alon, U.: Oscillations and variability in the p53 system. *Mol. Systems Biol.* 2 (2006)
20. Goldbeter, A.: Computational approaches to cellular rhythms. *Nature* 420, 238–245 (2002)
21. Gordon, K.E., Van Leeuwen, I.M.M., Lain, S., Chaplain, M.A.J.: Spatio-temporal modelling of the p53-mdm2 oscillatory system. *Math. Model. Nat. Phenom.* 4, 97–116 (2009)
22. Haupt, Y., Maya, R., Kazaz, A., Oren, M.: Mdm2 promotes the rapid degradation of p53. *Nature* 387, 296–299 (1997)
23. Hirata, H., Yoshiura, S., Ohtsuka, T., Bessho, Y., Harada, T., Yoshikawa, K., Kageyama, R.: Oscillatory expression of the Bhlh factor Hes1 regulated by a negative feedback loop. *Science* 298, 840–843 (2002)
24. Horvath, G., Dini, P.: Lie Group Analysis of p53-mdm3 Pathway. In: *Proceedings of the 3rd OPAALS International Conference, Aracaju, Sergipe, Brazil, March 22-23 (2010)*

25. Krishna, S., Jensen, M.H., Sneppen, K.: Minimal model of spiky oscillations in NF-KB. *Proc. Natl. Acad. Sci. USA* 103, 10840–10845 (2006)
26. Kruse, J.P., Gu, W.: Modes of p53 regulation. *Cell* 137, 609–622 (2009)
27. Lahav, G.: Oscillations by the p53-mdm2 feedback loop. *Adv. Exp. Med. Biol.* 641, 28–38 (2008)
28. Lahav, G., Rosenfield, N., Sigal, A., Geva-Zatorsky, N., Levine, A.J., Elowitz, M.B., Alon, U.: Dynamics of the p53-mdm2 feedback loop in individual cells. *Nat. Gen.* 36, 147–150 (2004)
29. Lane, D.P.: p53, guardian of the genome. *Nature* 358, 15–16 (1992)
30. Lev Bar-Or, R., Maya, R., Segel, L.A., Alon, U., Levine, A.J., Oren, M.: Generation of oscillations by the p53-mdm2 feedback loop: a theoretical and experimental study. *Proc. Natl. Acad. Sci. USA* 97, 11250–11255 (2000)
31. Levine, H.A., Smiley, M.W., Tucker, A.L., Nilsen-Hamilton, M.: A mathematical model for the onset of avascular tumor growth in response to the loss of p53 function. *Cancer Informatics* 2, 163–188 (2006)
32. Ma, L., Wagner, J., Rice, J.J., Hu, W., Levine, A.J., Stolovitzky, G.A.: A plausible model for the digital response of p53 to dna damage. *Proc. Natl. Acad. Sci. USA* 102, 14266–14271 (2005)
33. Mihalas, G.I., Simon, Z., Balea, G., Popa, E.: Possible oscillatory behaviour in p53-mdm2 interaction computer simulation. *J. Biol. Syst.* 8, 21–29 (2000)
34. Monk, N.A.M.: Oscillatory expression of hes1, p53, and NF-KB driven by transcriptional time delays. *Curr. Biol.* 13, 1409–1413 (2003)
35. Nelson, D.E., Ihekweba, A.E., Elliott, M., Johnson, J.R., Gibney, C.A., Foreman, B.E., Nelson, G., See, V., Horton, C.A., Spiler, D.G., Edwards, S.W., McDowell, H.P., Unitt, J.F., Sullivan, E., Grimley, R., Benson, N., Broomhead, D., Kell, D.B., White, M.R.: Oscillations in NF-KB signaling control de dynamics of gene expression. *Science* 306, 704–708 (2004)
36. Ogunnaike, B.A.: Elucidating the digital control mechanism for dna damage repair with the p53-mdm2 system: single cell data analysis and ensemble modelling. *J. R. Soc. Interface* 3, 175–184 (2006)
37. Pigolotti, S., Krishna, S., Jensen, M.H.: Oscillation patterns in negative feedback loops. *Proc. Natl. Acad. Sci. USA* 104, 6533–6537 (2007)
38. Proctor, C.J., Gray, D.A.: Explaining oscillations and variability in the p53-mdm2 system. *BMC Syst. Biol.* 2, 75 (2008)
39. Puszynski, K., Hat, B., Lipniacki, T.: Oscillations and bistability in the stochastic model of p53 regulation. *J. Theor. Biol.* 254, 452–465 (2008)
40. Ribba, B., Colin, T., Schnell, S.: A multiscale mathematical model of cancer, and its use in analyzing irradiation therapies. *Theor. Biol. Med. Model.* 3, 7 (2006)
41. Shieh, S.Y., Ikeda, M., Taya, Y., Prives, C.: DNA damage-induced phosphorylation of p53 alleviates inhibition by mdm2. *Cell* 91, 325–334 (1997)
42. Srividya, J., Gopinathan, M.S., Schnells, S.: The effects of time delays in a phosphorylation-dephosphorylation pathway. *Biophys. Chem.* 125, 286–297 (2007)
43. Tiana, G., Jensen, M.H., Sneppen, K.: Time delay as a key to apoptosis induction in the p53 network. *Eur. Phys. J. B* 29, 135–140 (2002)
44. Tiana, G., Krishna, S., Pigolotti, S., Jensen, M.H., Sneppen, K.: Oscillations and temporal signalling in cells. *Phys. Biol.* 4, R1–R17 (2007)
45. Tigges, M., Marquez-Lago, T.T., Stelling, J., Fussenegger, M.: A tunable synthetic mammalian oscillator. *Nature* 457, 309–312 (2009)

46. Vogelstein, B., Lane, D.P., Levine, A.J.: Surfing the p53 network. *Nature* 408, 307–310 (2007)
47. Wagner, J., Ma, L., Rice, J.J., Hu, W., Levine, A.J., Stolovitzky, G.A.: P53-mdm2 loop controlled by a balance of its feedback strength and effective dampening using atm and delayed feedback. *IEE Proc. Syst. Biol.* 152, 109–118 (2005)
48. Wawra, C., Kuhl, M., Kestler, H.A.: Extended analyses of the wnt β -cateni pathway: robustness and oscillatory behaviour. *FEBS Lett.* 581, 4043–4048 (2007)
49. Zauberman, A., Flusberg, D., Haupt, Y., Barak, Y., Oren, M.: A functional p53-response intronic promoter is contained within the human mdm2 gene. *Nucleic Acids Res.* 23, 2584–2592 (1995)
50. Zhang, T., Brazhnik, P., Tyson, J.J.: Exploring mechanisms of DNA damage response: p53 pulses and their possible relevance to apoptosis. *Cell Cycle* 6, 85–94 (2007)